

PAPER

Parametric Wind Velocity Vector Estimation Method for Single Doppler LIDAR Model

Takayuki MASUO^{†a)}, *Student Member*, Fang SHANG[†], Shouhei KIDERA[†], Tetsuo KIRIMOTO[†], Hiroshi SAKAMAKI^{††}, and Nobuhiro SUZUKI^{††}, *Members*

SUMMARY Doppler lidar (Light Detection And Ranging) can provide accurate wind velocity vector estimates by processing the time delay and Doppler spectrum of received signals. This system is essential for real-time wind monitoring to assist aircraft taking off and landing. Considering the difficulty of calibration and cost, a single Doppler lidar model is more attractive and practical than a multiple lidar model. In general, it is impossible to estimate two or three dimensional wind vectors from a single lidar model without any prior information, because lidar directly observes only a 1-dimensional (radial direction) velocity component of wind. Although the conventional VAD (Velocity Azimuth Display) and VVP (Velocity Volume Processing) methods have been developed for single lidar model, both of them are inaccurate in the presence of local air turbulence. This paper proposes an accurate wind velocity estimation method based on a parametric approach using typical turbulence models such as tornado, micro-burst and gust front. The results from numerical simulation demonstrate that the proposed method remarkably enhances the accuracy for wind velocity estimation in the assumed modeled turbulence cases, compared with that obtained by the VAD or other conventional method.

key words: *Light Detection and Ranging (lidar), single lidar model, local air turbulence estimation*

1. Introduction

Low-level windshear related to local turbulence is one of the main factors which can lead to aircraft accidents in landing or taking off [1]. Since the operation of real-time monitoring systems commenced with terminal Doppler wind radar (TDWR) at the beginning of the 1990s in the United States [2], a number of signal processing approaches for wind velocity measurement techniques using Doppler radar have been actively investigated [3], [4]. However, Doppler radar systems work only when it rains, because it requires an echo from raindrops. In recent years, the remote sensing technique with lidar (light detection and ranging) has entered into the spotlight as a technique for velocity estimation and wind shear detection [5]. Lidar measures the wind velocity by analyzing the echo scattered by atmospheric aerosols and molecules. Subsequently, not only for rainy weather, the lidar can be generally used in all weather conditions, except for heavy rain or snow fall. Basically, there are two opera-

tion modes of the lidar system. Multiple lidar systems can measure the general two dimensional(2-D) wind velocity in real atmospheric situation, however, operators suffer great difficulties for calibrating radial velocities in such system [6]–[8]. On the contrary, a single lidar system is considered preferable since it does not need complicated calibration or synchronization.

The velocity azimuth display (VAD) method is one of the most simple or useful models for the single lidar system [9]. The VAD method assumes that the wind has a constant speed and direction with the same range but different azimuth angles. This assumption makes it possible to calculate the 2-D velocity vector field using only a single-lidar model. However, in some cases, such as local air turbulence, with significant variation in local area, the VAD method yields inaccurate velocity vector estimations. As another approach for solving this problem, the velocity volume processing (VVP) method is developed based on linear approximation of velocity distribution in local spatial region [10]. However, in the case of non-linear distribution, this method does not achieve sufficient accuracy, naturally, due to assuming the linear-distribution. As a solution for this problem, we have already proposed the extended VAD method that adaptively changes the correlation area in the cost function [11]. While some cases show that the extended VAD method achieves better performance in estimating wind velocity than either VAD or VVP, it shows still room for improvement in local air turbulence estimation accuracy. As other literature, turbulence estimation and detection methods using a single lidar have been discussed, where the difficulty of developing accurate wind velocity estimation is demonstrated [12].

In an aircraft landing or taking off situation, since it is required for the operator to judge what kind of the local turbulences could occur along the aircraft path, it is rather important to recognize the typical local turbulences (e.g. gust front or tornado) with its location and scale from the observed Doppler velocity distributions, than to know the general 2-D velocity map. According to this background, this paper proposes the parametric window velocity estimation method for specific turbulence models, such as tornado or gust for single lidar model. Although the parametric approach for typical tornado model has been proposed using Ranking vortex model [13], it did not introduces the comparison or recognition of different kinds of turbulence. The proposed method introduces mathematical turbulence models, i.e., uniform distribution, tornado, microburst, and gust

Manuscript received July 6, 2016.

Manuscript revised September 14, 2016.

Manuscript publicized October 12, 2016.

[†]The authors are with Graduate School of Informatics and Engineering, The University of Electro-Communications, Chofu-shi, 182-8585 Japan.

^{††}The authors are with Information Technology R&D Center, Mitsubishi Electric Corporation, Kamakura-shi, 247-8501 Japan.

a) E-mail: masuo@secure.ee.uec.ac.jp

DOI: 10.1587/transcom.2016EBP3265

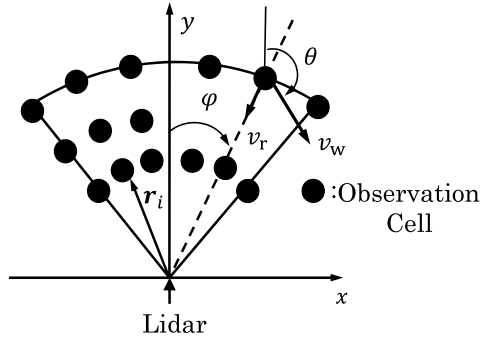


Fig. 1 System model.

front, and determines the optimum parameters by minimizing the residual errors between observed and estimated radial velocity discrepancy. In addition, this method has notable feature that an occurred air turbulence is directly and automatically determined in the process of optimization. To solve the multi-dimensional optimization problem, we employ the particle swarm optimization (PSO) is used here to avoid the local optimal solution [14]. The results of 2-D numerical analyses show that the proposed method achieves significantly higher accuracy in comparison with conventional methods with automatically selecting an appropriate turbulence model.

2. System Model

This paper assumes the 2-D problem in monostatic lidar observation. Figure 1 shows the system model. In this figure, each black circle denotes a resolution cell, whose size is determined by the range and azimuth resolution of lidar. The parameter v_r denotes the radial velocity, φ is the angle in the azimuth direction and θ is the angle of \mathbf{v} from the y axis. \mathbf{v} denotes a wind velocity vector with components $(v\sin(\theta), v\cos(\theta))$ in directions x and y . Wind vectors of the observation area are expressed by using such polar coordination model as (\mathbf{v}, θ) . It also assumes that the horizontal wind is invariant in the observed event.

3. Conventional Methods

This section introduces the three conventional approaches, which are typically used in single lidar issue.

3.1 VAD Method

The VAD method estimates a wind velocity vector, under the assumption that the velocity vector is invariant in an area of constant distance but varying in azimuth direction. The methodology of this method is briefly explained as follows. Here, r denotes the distance between the observation cell and lidar location. When the curve of the surface of the Earth is negligible, the radial velocity is defined as

$$v_r(r, \varphi) = \frac{1}{2}r \left(\frac{\partial u}{\partial x} + \frac{\partial v}{\partial y} \right) + v_0 \cos \varphi + u_0 \sin \varphi$$

$$+ \frac{1}{2}r \left(\frac{\partial v}{\partial y} - \frac{\partial u}{\partial x} \right) \cos 2\varphi + \frac{1}{2}r \left(\frac{\partial v}{\partial x} + \frac{\partial u}{\partial y} \right) \sin 2\varphi, \quad (1)$$

where (u, v) denotes x and y components of a wind vector \mathbf{v} in the spatial domain and (u_0, v_0) is a wind vector in the center of the correlation region. Assuming a uniform distribution in this correlation region, the partial differential terms of Eq. (1) can be eliminated and the radial velocity can be expressed as

$$v_r(v(\mathbf{r}_i), \theta(\mathbf{r}_i)) = v \cos(\theta - \varphi). \quad (2)$$

The wind velocity is estimated by minimizing the square mean of residuals as

$$\left(\hat{v}(\mathbf{r}_i), \hat{\theta}(\mathbf{r}_i) \right) = \underset{v(\mathbf{r}_i), \theta(\mathbf{r}_i)}{\operatorname{argmin}} \sum_{\mathbf{r}_i \in \Omega_i} \{v_r(v(\mathbf{r}_i), \theta(\mathbf{r}_i)) - v_{r, \text{obs}}(\mathbf{r}_i)\}^2, \quad (3)$$

where Ω_i denotes the correlation region centered on the observation cell \mathbf{r}_i and $v_{r, \text{obs}}(\mathbf{r}_i)$ denotes the observed radial velocity. Given that the VAD method assumes a uniform wind in the correlation region, its estimation accuracy is significantly degraded in the case of large variance in evaluating cells.

3.2 VVP Method

The VVP method calculates the wind velocity vector by making a linear approximation of the spatial variance of the wind field. Supposing (x_0, y_0) is the center location of the observed region, the wind vector $\mathbf{v}(x, y)$ of the location (x, y) is expanded by making the first-order approximation of a Taylor series expansion as,

$$\mathbf{v}(x, y) \approx \mathbf{v}(x_0, y_0) + \frac{\partial \mathbf{v}}{\partial x} (x - x_0) + \frac{\partial \mathbf{v}}{\partial y} (y - y_0). \quad (4)$$

The radial velocity can then be expressed as

$$v_r = \mathbf{v} \cdot (\mathbf{i}_x \sin \varphi + \mathbf{i}_y \cos \varphi) = \mathbf{P} \mathbf{K}, \quad (5)$$

where

$$\mathbf{P} = \begin{bmatrix} \sin \varphi \\ \cos \varphi \\ \sin \varphi (r \sin \varphi - x_0) \\ \cos \varphi (r \cos \varphi - y_0) \\ r \sin \varphi \cos \varphi \end{bmatrix}^T, \quad \mathbf{K} = \left(u_0', v_0', \frac{\partial u}{\partial x}, \frac{\partial v}{\partial y}, \left(\frac{\partial u}{\partial y} + \frac{\partial v}{\partial x} \right) \right)^T.$$

Parameter \mathbf{i}_x and \mathbf{i}_y are unit vectors in directions x and y respectively, $u_0' C v_0'$ are defined as $u_0' = u_0 - \frac{\partial u}{\partial y} y_0$ and $v_0' = v_0 - \frac{\partial v}{\partial x} x_0$. In general, the number of observation data n satisfies the condition $n \gg \operatorname{rank}(\mathbf{K})$. \mathbf{K} is calculated using the least-squares method of observed radial velocities. Parameter \mathbf{v}_r composed of n radial velocities is expressed by \mathbf{P} as $\mathbf{v}_r = \mathbf{P} \mathbf{K}$. The normal equation for \mathbf{K} is found from

$$\mathbf{K} = (\mathbf{P}^T \mathbf{P})^{-1} (\mathbf{P}^T \mathbf{v}_r). \quad (6)$$

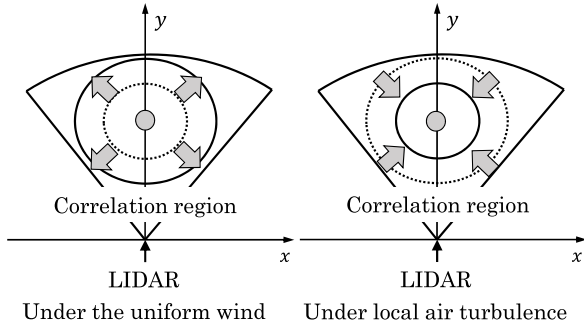


Fig. 2 Adaptive correlation length in the extended VAD method.

Parameter u_0' and v_0' obtained from Eq. (6) should include the rotation term. Since this method makes a linear approximation of the spatial variance of the wind field, in a nonlinear case such as turbulence, its accuracy degrades. In addition, because the difference operation is used in calculating the wind velocity, the method is, in general, much sensitive to fluctuations of the measurement errors.

3.3 Extended VAD Method

The main problem of the VAD and VVP methods is that assumption of both methods which the distribution in spatial domain is uniform or linear approximation becomes invalid under the local air turbulence. To overcome this problem, the literature [11] have extended the original VAD method by adaptively optimizing the spatial correlation length for the wind field calculation, i.e., the method optimizes not only the wind velocity vector but also the spatial correlation length $\sigma(\mathbf{r}_i)$. The three parameters are determined by

$$\begin{aligned} & (\hat{v}(\mathbf{r}_i), \hat{\theta}(\mathbf{r}_i), \hat{\sigma}(\mathbf{r}_i)) = \\ & \underset{v(\mathbf{r}_i), \theta(\mathbf{r}_i), \sigma(\mathbf{r}_i)}{\operatorname{argmin}} \frac{\sum_{\mathbf{r}_j \in \Omega_i} e^{-\frac{|\mathbf{r}_i - \mathbf{r}_j|^2}{2\sigma^2(\mathbf{r}_i)}} \{v_r(v(\mathbf{r}_i), \theta(\mathbf{r}_i)) - v_{r,\text{obs}}(\mathbf{r}_i)\}^2}{\sum_{\mathbf{r}_j \in \Omega_i} e^{-\frac{|\mathbf{r}_i - \mathbf{r}_j|^2}{2\sigma^2(\mathbf{r}_i)}}}, \end{aligned} \quad (7)$$

where $\sigma(\mathbf{r}_i)$ denotes the correlation length in the spatial domain. Ω_i denotes the correlation region centered on the observation cell \mathbf{r}_i . Figure 2 shows the adaptive correlation region according to the wind field. This method allows us to estimate the wind velocity in the case of local air turbulence by adaptively changing the spatial correlation length. It has been demonstrated that extended VAD method can provide more accurate estimation of wind vectors than the VAD and VVP methods, but it suffered from severe inaccuracy in the case of larger local variance cases, such as tornado or gust front [11].

4. Proposed Method

This section presents the principle and methodology of the proposed method. As previously mentioned, all the aforementioned conventional methods suffer from inaccuracy for

velocity estimation, in the case of local air turbulence. As a solution to this problem, this paper introduces a parametric approach by introducing the mathematical model for each turbulence pattern as follows.

(1) Uniform Distribution model

v and θ are constant at all observation cells. Then, the parameter vectors in this model is defined as $\mathbf{p}_1 = (v, \theta)$.

(2) Tornado model

The tornado is approximated using the Rankine vortex model [17] in which the wind velocity norm reaches a maximum v_c at a distance r_c from the center location. This model is expressed as

$$\|v\|(x, y) = \begin{cases} \frac{v_c}{r_c} d(x, y) & (d \leq r_c) \\ \frac{v_c r_c}{d(x, y)} & (d > r_c) \end{cases}, \quad (8)$$

where $d(x, y) = \sqrt{(x - x_c)^2 + (y - y_c)^2}$. (x_c, y_c) is the coordinates of the center locations of the tornado, and the wind direction is expressed as

$$\theta(x, y) = \tan^{-1} \left(\frac{x - x_c}{y - y_c} \right) + \frac{\pi}{2}. \quad (9)$$

Then, the parameter vectors in this model is defined as $\mathbf{p}_2 = (x_c, y_c, r_c, v_c)$.

(3) Microburst model

The microburst represents a downdraft, and generates a strong gust in the radial direction when it hits the ground. The wind velocity variation model of the microburst is similar to that of tornado model using the Rankine vortex model [18]. The wind direction is expressed as

$$\theta(x, y) = \tan^{-1} \left(\frac{x - x_c}{y - y_c} \right), \quad (10)$$

where $\|v\|$ is determined in Eq. (8). Then, the parameter vectors in this model is defined as $\mathbf{p}_3 = (x_c, y_c, r_c, v_c)$.

(4) Gust front model

The gust front is the updraft generated by the collision of air currents. The norm of the 2-D wind vector of this model is expressed as

$$\|v\|(x, y) = \begin{cases} v \cos \left(\tan^{-1} \left(-\frac{\sigma^2}{D(x, y)^2} \right) \right) & ((x, y) \in \Omega_1) \\ -v \cos \left(\tan^{-1} \left(-\frac{\sigma^2}{D(x, y)^2} \right) \right) & ((x, y) \in \Omega_2) \end{cases}, \quad (11)$$

where v denotes the constant coefficient, σ is the curvature coefficient of the wind velocity variation, and $D(x, y) = \sqrt{(x_c - x)^2 + (y_c - y)^2} - R$. Boundary of Ω_1 and Ω_2 is called shear line, and is drawn in a circle of radius R . The wind direction is expressed as

$$\theta(x, y) = \begin{cases} \tan^{-1} \left(\frac{x - x_c}{y - y_c} \right) & ((x, y) \in \Omega_1) \\ \tan^{-1} \left(\frac{x - x_c}{y - y_c} \right) - \pi & ((x, y) \in \Omega_2) \end{cases}. \quad (12)$$

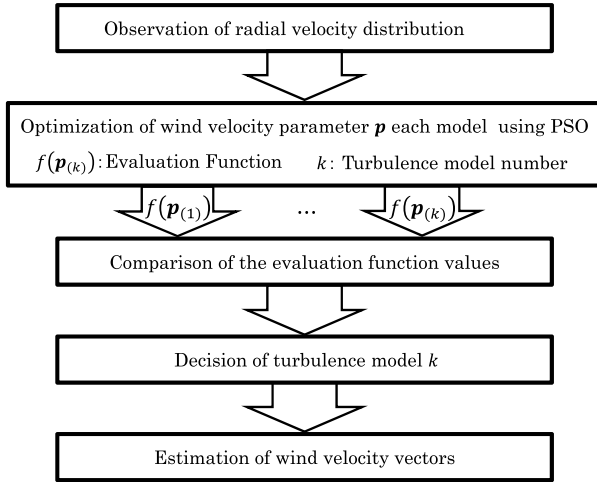


Fig. 3 Flowchart of the proposed method.

Then, the parameter vectors in this model is defined as $\mathbf{p}_4 = (x_c, y_c, R, v, \sigma)$.

Using the above mathematical wind model, the turbulence model denoted is determined as;

$$\hat{k} = \operatorname{argmin}_k \left(\min_{\mathbf{p}_k} \sum_{\mathbf{r}_j \in \Omega} (v_{r,\text{est}}(\mathbf{p}_k) - v_{r,\text{obs}}(\mathbf{r}_j))^2 \right), \quad (13)$$

where k denotes the index number of turbulence model, Ω denotes all the observation region and \mathbf{p}_k denotes parameter vector in the k th turbulence model, which includes the location or scale of each turbulence. $v_{r,\text{est}}(\mathbf{p}_k)$ is the calculated radial velocity from k th turbulence model. This method automatically selects the most appropriate model by evaluating the radial velocity, and offers accurate estimation with a small number of optimization variables. In this case, to avoid the local optimization problem, the PSO algorithm is introduced in this optimization [14]. Furthermore, this paper introduces the network structure into the PSO algorithm to improve a convergence performance [15], [16]. Figure 3 shows the flowchart of the proposed method.

5. Performance Evaluation in Numerical Simulations

This section describes results of the numerical simulation conducted for performance analysis. In these simulations, 21 and 11 cells are sampled in the range and azimuth directions, respectively. The observation interval is 150 m in the range direction and 6° in the azimuth direction at the range of $-30^\circ \leq \varphi \leq 30^\circ$. Note that, the characteristic of synoptic-, meso-, and local-scale meteorological phenomena is time dependent, naturally. However, it is considered that this time variance effect is negligible within an updating time of lidar, because the beam scanning velocity of lidar is estimated as 10 deg/sec, indicating that the updating rate for wind vector fields for 60 degree azimuth range is less than 10 sec. Since the average motion velocity of tornado is in the range between 10 and 20 meters, the motion amount in

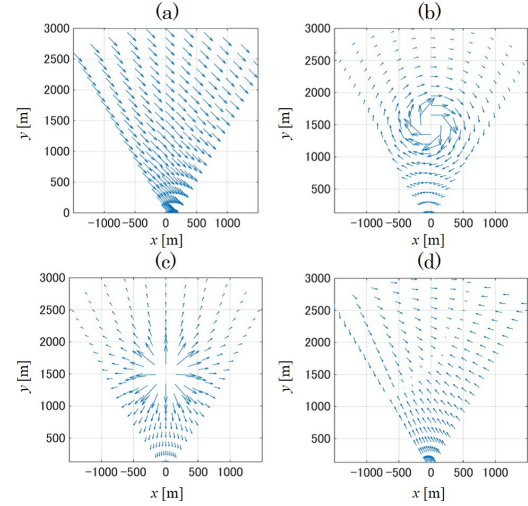


Fig. 4 True wind vectors ((a): uniform distribution, (b): tornado, (c): microburst and (d): gust front).

updating interval is estimated around 60 m, which is within the range resolution (150 m in this case). Then, we regard that the variance of center location or size of each turbulence could be ignored in this case. We assess the performance of the proposed method for four wind field models as uniform distribution, tornado, microburst and gust front. These turbulences greatly affect the safety of aircraft navigation.

True wind vectors in each wind field model are shown in Fig. 4. True parameters of each wind field model are set to $\mathbf{p}_1 = (v, \theta) = (10 \text{ m/s}, 135^\circ)$, $\mathbf{p}_2 = (x_c, y_c, r_c, v_c) = (0 \text{ m}, 1500 \text{ m}, 200 \text{ m}, 20 \text{ m/s})$, $\mathbf{p}_3 = (x_c, y_c, r_c, v_c) = (0 \text{ m}, 1500 \text{ m}, 200 \text{ m}, 20 \text{ m/s})$, $\mathbf{p}_4 = (x_c, y_c, R, v, \sigma) = (-1500 \text{ m}, 3000 \text{ m}, 2000 \text{ m}, 5 \text{ m/s}, 140 \text{ m})$ respectively. Figures 5, 6, 7 and 8 present the wind vector estimated using the VAD, VVP, the extended VAD and proposed methods, respectively, in noiseless situation. Here, in the case of the original VAD, each cell denoted as \mathbf{r}_i is evaluated by using two neighboring cells (denoted as Ω_i in Eq. (3)) along the azimuth direction at the same range. Also, in the VVP method, each cell is evaluated by four neighboring cells along range and azimuth directions. In PSO algorithm, we set a number of particle, replication and network-bound particles as 500, 200 and 3 respectively. In particular, the estimation errors of tornado and microburst, in the far range regions, are significantly reduced by the proposed method, while the other methods suffer from the significant inaccuracy in such case.

For quantitative analysis of the estimation accuracy of the wind field, the normalized root mean square error (NRMSE) is introduced as

$$\text{NRMSE} = \sqrt{\frac{\sum_{i=1}^N |\mathbf{v}_{\text{true}} - \mathbf{v}_i|^2}{\sum_{i=1}^N |\mathbf{v}_{\text{true}}|^2}}, \quad (14)$$

where N denotes the number of observation cells, and \mathbf{v}_{true} and \mathbf{v}_i are true wind vectors and estimated wind vectors, respectively. Table 1 gives the NRMSE for each method. Table 1 shows that, in comparison with the VAD, VVP and the extended VAD methods, the proposed method achieves

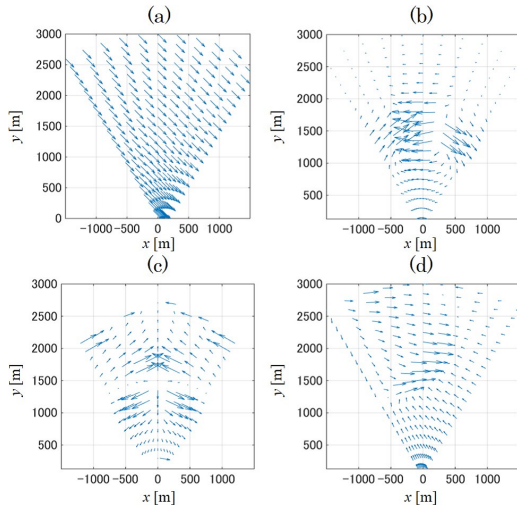


Fig. 5 Estimation results with VAD method ((a): uniform distribution, (b): tornado, (c): microburst and (d): gust front).

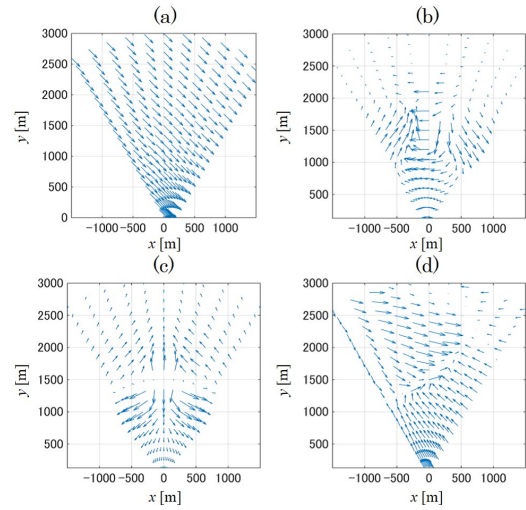


Fig. 7 Estimation results with the extended VAD method ((a): uniform distribution, (b): tornado, (c): microburst and (d): gust front).

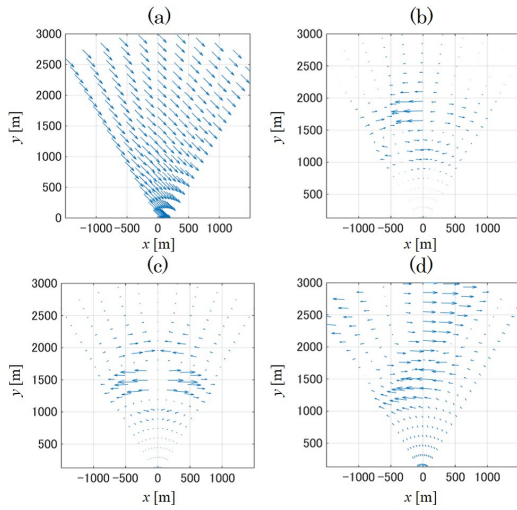


Fig. 6 Estimation results with VVP method ((a): uniform distribution, (b): tornado, (c): microburst and (d): gust front).

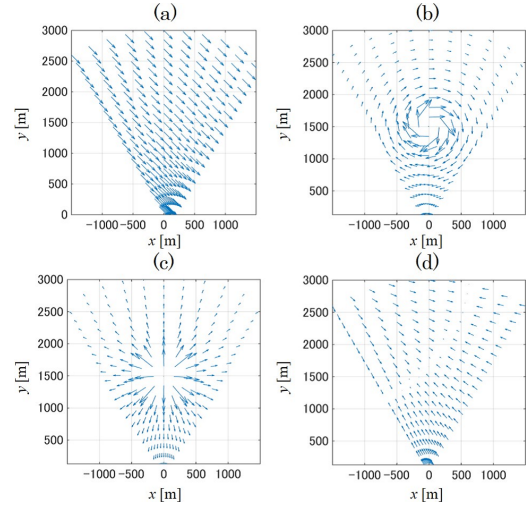


Fig. 8 Estimation results with the proposed method ((a): uniform distribution, (b): tornado, (c): microburst and (d): gust front).

significantly lower NRMSE for the tornado, microburst, and gust front models. The estimation accuracy of gust front is slightly degraded to other models because, in this model, the number of parameters in mathematical model, namely, optimization variables, is larger than that of other models.

Next, we consider the effect of random fluctuations on the measurement of the radial velocity, namely the evaluation in noisy situation. Lidar steadily includes fluctuation on radial velocity as measurement equipment error. Since the SNR for each observation data significantly depends on a selected filtering process or the assumed type of random noises (Gaussian or others), we directly add the fluctuation to observed radial velocity based on the actual lidar measurement, for simplicity. We add the fluctuation Δv_r for the observed radial velocity, whose probability density function follows a Gaussian distribution. Standard deviation of this Gaussian fluctuation ζ is varied between 0.2 m/s and 1.0 m/s.

Table 1 NRMSE in each wind field model.

	Uniform Wind	Tornado	Microburst	Gust Front
VAD	6.50×10^{-3}	1.36	1.79	0.988
VVP	1.25×10^{-7}	7.45	6.15	3.41
Ex. VAD	6.50×10^{-3}	0.761	1.04	0.713
Proposed	3.31×10^{-4}	0.166	0.162	0.191

Figure 9 shows the NRMSE versus ζ . This figure show that each NRMSE rapidly increases with increasing standard deviation of the fluctuation ζ in the conventional methods. In contrast, the proposed method remarkably suppress the accuracy degradation even in more fluctuated cases.

Next, we assess effect of fluctuations on assumed mathematical model. Since the natural wind includes the fluctuation of the wind velocity vector, to reproduce this case by adding the fluctuation in the parameters that constitute the wind velocity vector field, that is to say, the exact solution

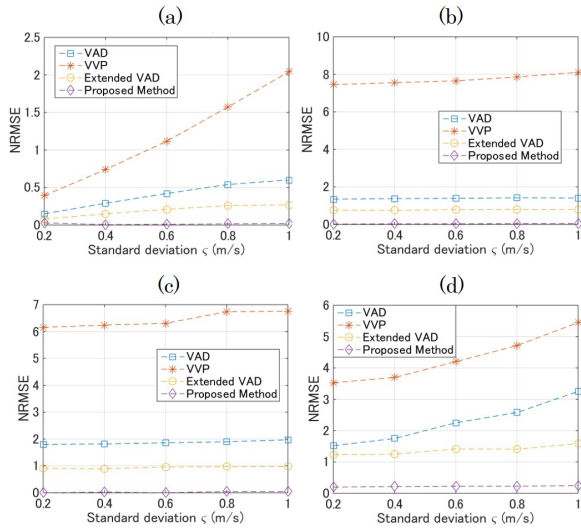


Fig. 9 The NRMSE versus ς_n ((a): uniform distribution, (b): tornado, (c): microburst and (d): gust front).

Table 2 Standard deviation of Δp_k for each parameter.

Turbulence type	p_k	S.D of Δp_k
Uniform Wind	(v, θ)	(5 m/s, 10 deg.)
Tornado	(x_c, y_c, r_c, v_c)	(150 m, 150 m, 100 m, 10 deg.)
Microburst	(x_c, y_c, r_c, v_c)	(150 m, 150 m, 100 m, 10 deg.)
Gust Front	(x_c, y_c, R, v, σ)	(150 m, 150 m, 20 m, 5 m/s, 30 m)

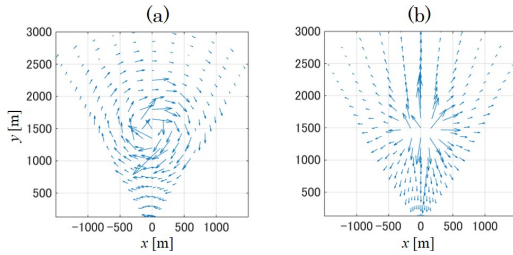


Fig. 10 Estimation results in parameter fluctuations ((a): tornado, (b): microburst).

Table 3 NRMSE in each wind field model with parameter fluctuations.

	Uniform Wind	Tornado	Microburst	Gust Front
VAD	0.654	1.95	1.99	1.67
VVP	2.51	6.94	6.34	4.25
Ex. VAD	0.493	1.57	1.34	1.04
Proposed	0.108	0.418	0.471	0.425

for the turbulence parameters depends on the location of observation cell. The parameter vectors including fluctuations expressed as $\hat{p}_k = p_k + \Delta p_k$, where Δp_k denotes an error vector from actual one. Table 2 denotes the standard deviation of Δp_k for each model, in this case. The left side and right side of Fig. 10 show the examples for the cases of tornado and microburst wind vectors by the proposed method, where parameter fluctuations in Table 2 are given. Table 3 gives the NRMSE for each method in this case, and even in the case that a unique solution does not exist.

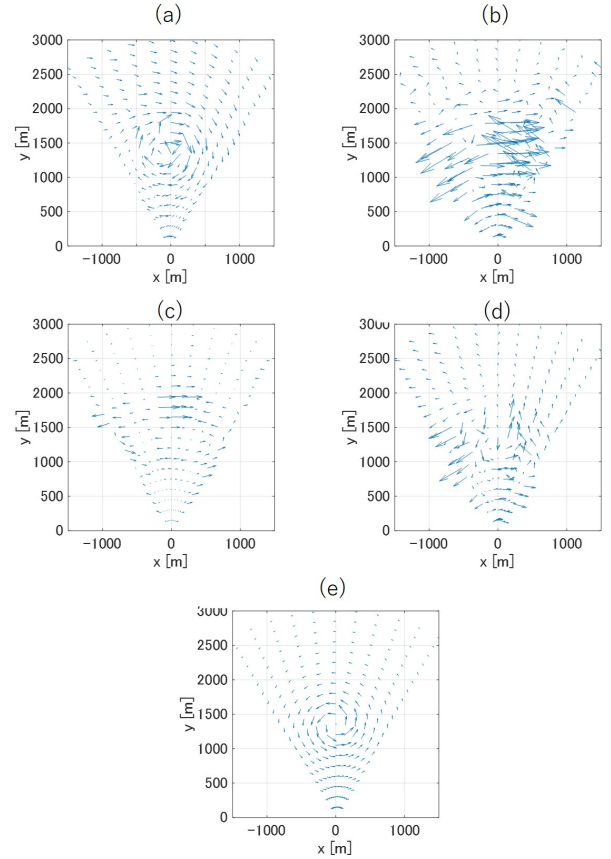


Fig. 11 Estimation results of window velocity with mixture models ((a): Actual, (b): VAD, (c): VVP, (d): extended VAD and (e): proposed method).

Finally, to test more general case, the case where multiple turbulence models are mixed together, is investigated for revealing the relevance of the proposed method. Here, the actual distribution of the window velocity vector field $v(x, y)$ is expressed as the linear combination of each turbulence model as;

$$v(x, y) = w_{\text{uni}}v_{\text{uni}}(x, y; p_1) + w_{\text{tor}}v_{\text{tor}}(x, y; p_2) + w_{\text{micro}}v_{\text{micro}}(x, y; p_3) + w_{\text{gust}}v_{\text{gust}}(x, y; p_4). \quad (15)$$

Figure 11 shows the examples of this mixture model for each method, where $(w_{\text{uni}}, w_{\text{tor}}, w_{\text{micro}}, w_{\text{gust}}) = (0.2, 0.5, 0.1, 0.2)$, that is, the tornado field is relatively dominant. True parameters of each wind field model are set to $p_1 = (v, \theta) = (10\text{m/s}, 135^\circ)$, $p_2 = (x_c, y_c, r_c, v_c) = (0\text{ m}, 1500\text{ m}, 200\text{ m}, 20\text{ m/s})$, $p_3 = (x_c, y_c, r_c, v_c) = (0\text{ m}, 1500\text{ m}, 200\text{ m}, 20\text{ m/s})$, $p_4 = (x_c, y_c, R, v, \sigma) = (-1500\text{ m}, 3000\text{ m}, 2000\text{ m}, 5\text{ m/s}, 140\text{ m})$ respectively. Here, the proposed method judges the dominant turbulence is ‘‘tornado’’ by comparing the cost functions in Eq.(13) among all possible turbulences. The estimated parameter of tornado model is $\hat{p}_2 = (8.9\text{ m}, 1453\text{ m}, 196\text{ m}, -10\text{ m/s})$. The NRMSEs for each method in this case are 2.75 for the VAD method, 6.84 for the VVP method, 1.864 for the extended VAD method and 1.61 for the proposed method, respectively. This results show that our method has the least error in this mixture

model. To enhance the accuracy in this method, it is promising to determine each weight value in the optimization, but it also requires more calculation time in the PSO optimization. Those problems should be treated in our future works.

6. Conclusion

This paper has proposed an accurate wind vector estimation method based on parametric estimation using four mathematical turbulence models. The results of numerical simulations have shown that the proposed method has higher accuracy in estimating the wind vector than conventional methods. In addition, it is found that the proposed method offers greater robustness to fluctuations on the measurement of the radial velocity and wind model. Note that, in the simulation of this study, the range cell resolution is set to 150 m, but in the case of smaller scale of meteorological phenomena, such cell resolution is not enough to determine the parameters accurately as less data is compared to unknowns (the degree of freedom of parameter p). However, the actual lidar measurements demonstrated higher range resolution of around 25 m, then, if the scale of local turbulence is smaller than 100 m, enough number of observation cells is available by using such higher range resolution lidar system. Since a coherent Doppler wind lidar uses a pulse laser with a long pulse width, we need to consider the trade-off between range and frequency resolutions in this case, which depend on the sampling frequency and sampling point. In addition, even in the case that the local turbulence, such as tornado, would shield the scattering echo from a target behind this turbulence, it is considered that the proposed method would work by exploiting the observable data from the vicinity area. To confirm the above discussion, it is necessary to investigate the real observation data. It should be noted that since the literature [13] using the same Ranking vortex model successfully estimates the actual wind field, it is predicted that the proposed method will also work well even in realistic scenario.

References

- [1] T.T. Fujita and F. Caracena, "An analysis of three weather-related aircraft accidents," *Bull. Am. Meteorol. Soc.*, vol.58, pp.1164–1181, Nov. 1977.
- [2] US Department of Transportation, FAA, "Terminal Doppler weather rader," Specification, FAA-E-2806b, Nov. 1989.
- [3] T.T. Fujita, "The downburst: Microburst and macroburst," SMRP Res. Rep, University of Chicago, June 1985.
- [4] J. Wurman and E. Rasmussen, "Fine-scale Doppler radar observations of tornadoes," *Science*, vol.272, pp.1774–1777, June 1996.
- [5] C.M. Shun and P.W. Chan, "Applications of an infrared Doppler lidar in detection of wind shear," *J. Atmos. Oceanic Technol.*, vol.25, pp.637–655, May 2008.
- [6] E.A. Brandes, "Flow in severe thunderstorms observed by dual-Doppler radar," *Bull. Am. Meteorol. Soc.*, vol.105, pp.113–120, Jan. 1977.
- [7] R. M. Lhermitte, "Dual-Doppler radar observations of convective storm circulation," *Proc. 14th Conf. Radr Meteor., Amer. Mereor. Soc.*, pp.139–144, 1970.
- [8] K. Traumnner, Th. Damian, Ch. Stawiarski, and A. Wieser, "Turbulent structures and coherence in the atmospheric surface layer" *Boundary-Layer Meteorol.*, vol.154, no.1, pp.1–25, 2015.
- [9] K.A. Browning and R. Wexler, "The determination of kinematic properties of a wind field using Doppler radar," *J. Appl. Meteorol.*, vol.7, no.1, pp.105–113, Feb. 1968.
- [10] P. Waldteufel and H. Corbin, "On the analysis of single Doppler radar data," *J. Appl. Meteorol.*, vol.18, no.4, pp.532–542, Feb. 1979.
- [11] T. Masuo, S. Kidera, T. Kirimoto, H. Sakamaki, and N. Suzuki, "Accurate wind velocity estimation method with single Doppler LIDAR model," IEICE Technical Report, SANE 114(264), pp.167–171, Oct. 2014.
- [12] A. Sathe, J. Mann, J. Gottschall, and M.S. Courtney, "Can wind lidars measure turbulence?," *J. Atmos. Oceanic Technol.*, vol.28, no.7, pp.853–868, July 2011.
- [13] C. Fujiwara, K. Yamashita, M. Nakanishi, and Y. Fujiyoshi, "Dust devil like vortices in an urban area detected by a 3D scanning Doppler lidar," *J. Appl. Meteor. Climatol.* vol.50, no.3, pp.534–547, 2011.
- [14] J. Kennedy and R. Eberhart, "Particle swarm optimization," *IEEE International Conference on Neural Networks*, vol.4, pp.1942–1948, 1995.
- [15] J. Kennedy and R. Mende, "Population structure and particle swarm performance," *IEEE Congress on Evolutionary Computation*, vol.2, pp.1671–1676, 2002.
- [16] T. Tsujimoto, T. Shindo, and K. Jin'no, "The neighborhood of canonical deterministic PSO," *Proc. IEEE Congr. Evol. Comput.*, pp.1937–1944, July 2011.
- [17] C.A. Wan and C.C. Chang, "Measurement of the velocity field in a simulated tornado-like vortex using a three-dimensional velocity probe," *J. Atmos. Sci.*, vol.29, no.1, pp.116–127, June 1972.
- [18] M.R. Hjelmfelt, "Structure and life circle of microburst outflows observed in Colorado," *J. Appl. Meteorol.*, vol.27, no.8, pp.900–927, Aug. 1988.



Takayuki Masuo received his B.E. degrees in Electronic Engineering from University of Electro-Communications in 2014. He is currently studying M.E degree at the Graduate School of Informatics and Engineering, University of Electro-Communications. His current research interest is advanced information processing of LIDAR application.



Fang Shang received the B.S. and M.S. degree in electrical engineering and automation from Harbin Institute of Technology, China, in 2009 and 2011. She received the Ph.D. degree in electrical engineering and information systems from The University of Tokyo, Japan, in 2014. She is an Assistant Professor in the Graduate School of Informatics and Engineering, University of Electro-Communications, Japan. Her current research interest is in the signal and imaging processing for the polarimetric SAR

and the UWB radar.



Shouhei Kidera received his B.E. degree in Electrical and Electronic Engineering from Kyoto University in 2003 and M.I. and Ph.D. degrees in Informatics from Kyoto University in 2005 and 2007, respectively. He is currently an Associate Professor in Graduate School of Informatics and Engineering, the University of Electro-Communications, Japan. His current research interest is in advanced radar signal processing or electromagnetic inverse scattering issue for ultra wideband (UWB) sensor. He was

awarded Ando Incentive Prize for the Study of Electronics in 2012, Young Scientists Prize in 2013 by the Japanese Minister of Education, Culture, Sports, Science and Technology (MEXT), and Funai Achievement Award in 2014. He is a member of the Institute of Electrical and Electronics Engineering (IEEE) and the Institute of Electrical Engineering of Japan (IEEJ).



Tetsuo Kirimoto received the B.S. and M.S. and Ph.D. degrees in Communication Engineering from Osaka University in 1976, 1978 and 1995, respectively. During 1978–2003 he stayed in Mitsubishi Electric Corp. to study radar signal processing. From 1982 to 1983, he stayed as a visiting scientist at the Remote Sensing Laboratory of the University of Kansas. From 2003 to 2007, he joined the University of Kitakyushu as a Professor. Since 2007, he has been with the University of Electro-Communications, where

he is a Professor at the Graduate School of Informatics and Engineering. His current study interests include digital signal processing and its application to various sensor systems. Prof. Kirimoto is a senior member of IEEE and a member of SICE (The Society of Instrument and Control Engineers) of Japan.



Hiroshi Sakamaki received the B.S. and M.S. degrees in Information Engineering from Hokkaido University in 1996 and 1998, respectively. He joined Mitsubishi Electric Corporation in 1998, where he has been engaged in research and development on radar signal processing for meteorological observations.



Nobuhiro Suzuki received the B.S. and M.S. in Electrical and Electronic Engineering from Tokyo Institute of Technology in 1992 and 1994 respectively. He has been working in Mitsubishi Electric Corp. since 1994 to study signal processing for radars, directional finders and location systems. He stayed as a graduate student in University of Alaska Fairbanks (UAF) from 1998 to 2001 and received Ph.D. degree in interdisciplinary of Science and Engineering in 2006. Nobuhiro Suzuki is a member of IEEE

and IEICE.